

# Visualizing cytoskeleton dynamics in mammalian cells using a humanized variant of monomeric red fluorescent protein

Markus Fischer<sup>a,\*</sup>, Ilka Haase<sup>a</sup>, Sebastian Wiesner<sup>b</sup>, Annette Müller-Taubenberger<sup>b,1</sup>

<sup>a</sup> *Lehrstuhl für Organische Chemie und Biochemie, Technische Universität München, Lichtenbergstr. 4, D-85747 Garching, Germany*  
<sup>b</sup> *Max-Planck-Institut für Biochemie, Am Klopferspitz 18, D-82152 Martinsried, Germany*

Received 7 March 2006; accepted 27 March 2006

Available online 17 April 2006

Edited by Jesus Avila

**Abstract** Fluorescent proteins are versatile tools for live cell imaging studies. In particular, recent progress was achieved in the development of monomeric red fluorescent proteins (mRFPs) that show improved properties in respect to maturation and intracellular fluorescence. mRFPmars, a red fluorescent protein designed especially for the use in *Dictyostelium*, proved to be a brilliant label for different cytoskeletal elements. Here we report on the synthesis of a humanized version of a monomeric RFP, mRFPruby, which differs in sequence from mRFPmars in four amino acids and has a codon usage that is optimized for the application in mammalian cells. In order to demonstrate the usefulness of this new mRFP variant, mRFPruby fused to  $\beta$ -actin was expressed in different mouse cell lines and used to visualize actin cytoskeleton dynamics by live cell microscopy. © 2006 Federation of European Biochemical Societies. Published by Elsevier B.V. All rights reserved.

**Keywords:** Actin cytoskeleton; Codon usage; Chondrocytes; Fluorescent protein; Monomeric RFP; mRFPruby; NIH 3T3; Synthetic gene

## 1. Introduction

Genetically encoded fluorescent proteins are now widely used as markers that allow visualizing the distribution of individual proteins or highlighting of cellular compartments [1,2]. In addition to visualize localization or to track redistribution, aspects of protein dynamics and interaction of specific components can be studied within living cells. Naturally occurring fluorescent proteins like the *Aequorea victoria* green fluorescent protein (GFP) [3] or variants of it as well as the advent of new fluorescent proteins [4,5] now offer researchers a full palette of fluorescent markers suitable for live cell imaging studies.

Proteins emitting in the red or far-red range are particularly useful, because they show reduced autofluorescence in eukaryotic cells. In addition, since the emission spectra of red fluorescent proteins (RFPs) can be clearly separated from GFP, they are also ideally suited for use in multicolor labeling. The first generation of RFPs was derived from the coral *Discosoma*.

These fluorescent labels, denoted as DsRed [6–8], and variants of it have the disadvantage of being obligate tetramers and are characterized by slow maturation and relatively weak fluorescence. However, consecutive runs of mutagenesis of DsRed and selection of stronger fluorescing variants led to the identification of RedStar, having seven altered amino acids [9]. By sequential mutagenesis of DsRed, a monomeric RFP, mRFP1, was obtained [10]. Another new version of mRFPs, mRFPmars [11], was originally designed for the use in *Dictyostelium* live cell imaging studies. For this purpose, a synthetic gene was produced that encoded a derivative of DsRed that combined the mutations that made the protein brighter [9], and monomeric [10], and employed the highly A/T-rich codon usage found in the genome of *Dictyostelium* [12]. mRFPmars turned out to be a brilliant fluorescence tag for various proteins in *Dictyostelium* [11,13], however, it was not suitable for expression in combination with other proteins in different mammalian cell lines (unpublished observations).

To overcome this insufficiency, we synthesized a RFP-gene encoding a protein with the amino acid sequence of *Dictyostelium* mRFPmars, but based on the codon usage found in humans. During the screen for correct clones in bacteria, several mutations of the original sequence of mRFPmars were obtained in addition to the humanized mRFPmars sequence. One of these clones, mRFPruby, had four additional amino acid changes when compared to the original mRFPmars amino acid sequence. We have tested the humanized variant mRFPruby in combination with  $\beta$ -actin in different mouse cell lines. mRFPruby- $\beta$ -actin turned out to be a suitable label to visualize the different actin structures observed in mammalian cells.

## 2. Materials and methods

### 2.1. Materials, bacterial strains and plasmids

Restriction enzymes and T4 DNA ligase were from New England Biolabs. EXT DNA Polymerase and Taq polymerase were from Finnzymes (Epsöo, Finland). Oligonucleotides were synthesized by Thermo Electron GmbH (Ulm, Germany). DNA fragments were purified with the CP-Kit, Gel Extraction Kit or Miniprep Kits from Peqlab (Erlangen, Germany) or Qiagen (Hilden, Germany). Polyclonal anti-actin antibody was purchased from Sigma (A 2066).

Unless otherwise stated, bacteria were grown at 37 °C in LB medium containing 170 mg ampicillin per l.

### 2.2. Sequence adaptation

The amino acid sequence corresponding to mRFPmars [11] was optimized using the program package DNAWorks (<http://mcl1.ncifcrf.gov/dnaworks/dnaworks2.html>), which reverse-translated the protein sequence using the codon frequency table for *Homo sapiens*

\*Corresponding author. Fax: +49 89 28913363.

E-mail address: markus.fischer@ch.tum.de (M. Fischer).

<sup>1</sup> Present address: Institut für Zellbiologie (ABI), Ludwig-Maximilians-Universität München, Schillerstr. 42, D-80336 München, Germany.

[14]. Flanking sequences were added for cloning of the optimized gene sequence. The algorithm of the program was used to divide the optimized gene sequence into 36 sections, which were characterized by an average annealing temperature of 58 °C and a maximum length of 50 bases (Table 1). The codon frequency threshold was set to 50%.

### 2.3. Gene assembly, amplification, and cloning

Oligonucleotides were obtained on a 20-nmol scale with standard RP-HPLC purification. Stock solutions were prepared at a concentration of 100 μM in water. Equal volumes of stock solutions were mixed together and diluted to a concentration of 2.5 μM. 1 μl of the mixed primers was employed in a PCR. The final concentrations of components were 25 nM of each oligonucleotide, 750 mM Tris/HCl, pH 9.0, 200 mM (NH<sub>4</sub>)<sub>2</sub>SO<sub>4</sub>, 0.1% (w/v) Tween 20, 15 mM MgCl<sub>2</sub>, 0.2 mM for each dNTP and 1 U of EXT Polymerase. The PCR protocol for gene assembly started with a 5-min denaturation step at 95 °C, followed by 25 cycles of denaturation at 95 °C for 30 s, annealing at 58 °C for 30 s and extension at 72 °C for 1 min. The last step was an incubation cycle at 72 °C for 2 min. 1 μl of this PCR product served as template, and the two flanking oligonucleotides HSRFP-1FW and HSRFP-1RV were used as primers in a subsequent 25-cycle amplification reaction (Fig. 1A).

The resulting 750-bp DNA-fragment was digested with *EcoRI* and *BglII*, subsequently cloned into the expression plasmid pNCO113 [15] (*EcoRI/BamHI*), and transformed into *Escherichia coli* strain XL-1 Blue [16] resulting in the recombinant strain XL-1-pNCO-HSmRFPmars. After the selection of brilliant red colored colonies, plasmids were purified and sequenced (GATC Biotech, Konstanz, Germany).

### 2.4. Expression and purification of humanized mRFPmars and mRFPruby

Plasmids isolated from the strain XL-1-pNCO-HSmRFPmars-7 (further designated as mRFPruby) and XL-1-pNCO-HSmRFP-8 (further designated as humanized mRFPmars) were transformed in *E. coli* M15 [pREP4] cells [17] and cultivated under shaking conditions at 37 °C in LB medium containing 170 mg ampicillin and 20 mg kanamycin per l up to an optical density of 0.6 at 600 nm. Isopropyl-β-D-thiogalactoside (IPTG) was added to a final concentration of 2 mM, and incubation was continued overnight. The bacteria were harvested by centrifugation, washed with 0.9% NaCl and stored at –20 °C.

Bacterial pellets were suspended in 50 mM Tris/HCl, pH 8.5 (buffer A), cooled on ice and ultrasonicated. After centrifugation (13000 rpm, 15 min, 4 °C), ammonium sulfate was added to the supernatant to a final concentration of 1.0 M. The solution was placed on top of a Phenyl-Sepharose column (1.6 × 10 cm, Amersham Pharmacia Biotech, Freiburg, Germany), equilibrated with buffer A containing 1.0 M ammonium sulfate. The column was developed with a linear gradient of 1.0–0 M ammonium sulfate in buffer A. Fractions were analyzed by SDS gel electrophoresis. Fractions containing humanized mRFPmars or mRFPruby, respectively, were combined and concentrated by ultrafiltration. The protein solution was desalted using a HiPrep desalting column (2.6 × 10 cm, Amersham Pharmacia Biotech), and placed on top of a Source-15Q column (1.0 × 10 cm, Amersham Pharmacia Biotech), which was equilibrated with buffer A. The column was developed with a linear gradient of 0–1.0 M KCl in buffer A. Fractions were combined, concentrated by ultrafiltration, and the protein solution was loaded on top of a Superdex 75 column (2.6 × 60 cm, Amersham Pharmacia Biotech) and eluted with 50 mM Tris/HCl, pH 7.5, containing 100 mM potassium chloride. mRFP containing red-colored fractions were combined and concentrated.

Table 1

Oligonucleotides used for the construction of the synthetic gene encoding humanized mRFPmars

Designation	Sequence (5' to 3')	Length
HSRFP-1FW	ataatagaattcattaaagaggagaaatctaactatgggcaa	41
HSRFP-2FW	gcttacatgcccagctccgaggatgcatcaaaagagtttatga	44
HSRFP-3FW	gatttaaggtcaagatggagggaagcgtcaacggacaoca	40
HSRFP-4FW	gttcgagattgaggagaaaggagaaggccggccttac	37
HSRFP-5FW	gagggcacacaaaaccgctaagctcaaggctcaaaaagga	39
HSRFP-6FW	ggaccctccctctcctcctgggataatcttgagcc	34
HSRFP-7FW	ctcagttccagtagcgaagcaaacgctatgtgaaacacccct	41
HSRFP-8FW	gccgacatccctgactatctgaagctctcctcctcctgaa	39
HSRFP-9FW	ggcttcaagtgaggagagaatcatgaacttcgaggacggga	39
HSRFP-10FW	ggcgtgggtgacagtcacacaagatagcaccctccaa	36
HSRFP-11FW	gacggagagtttatttataaagggtgaaactcagaggaaccaactcccc	48
HSRFP-12FW	tccgatggcctctgcatgcaaaaaaaaaacaatgggatgg	39
HSRFP-13FW	gaagcctccacogagagaatgtatcctgaggatggcg	37
HSRFP-14FW	ctctgaaaggcgaatataaaatgagactgaaactcaaaagacggagga	47
HSRFP-15FW	cactacgatgocgaggtcaaaaacaacctacaaggccaaga	40
HSRFP-16FW	aaacaagtgcagctgcccggcctacaagacagatatataa	41
HSRFP-17FW	ctcgacattatcagccataatgaggactacaccatcgtggaacaata	48
HSRFP-18FW	gagagagctgagggcagacatagcacaggcgcctggatcc	34
HSRFP-1RV	tattatataagatcttattatggatccagcgcctgtgctatg	42
HSRFP-2RV	tctgcccctcagctctctcatalatgttccacgatgggtgtagtc	42
HSRFP-3RV	ctcattatggctgataatgtcaggttataatctctgtctgtaggcgc	48
HSRFP-4RV	aggcagctgcacttgtttcttggcctttaggttgtttt	39
HSRFP-5RV	gacctcggcatogtagtctcctcctcctctttgagtttcag	39
HSRFP-6RV	tctcattttaatttcgctttcagagcgcctcctcaggatacatt	46
HSRFP-7RV	ctctcgggtggaggcctcccatcccatgtttttttttgca	40
HSRFP-8RV	tgacagggccatcggagggggaagtgggttcctctg	35
HSRFP-9RV	agtttcacctataaaataaaactctcctccttggagggtgctatccttgtg	49
HSRFP-10RV	tgactgtcaccacgcctcctcctcctcgaagttcctag	35
HSRFP-11RV	attctctcccacttgaagccttcagggaaggagagcttca	40
HSRFP-12RV	gatagtcagggatgtcggcagggtgtttcacataggcttt	40
HSRFP-13RV	gcttcgtaactggaactgagggtcagaataatcccaggc	39
HSRFP-14RV	gaaggggaggggctcctccttttgtgaacttgagcttag	38
HSRFP-15RV	cggtttgtgtgccctcgtaaaggccggccttct	32
HSRFP-16RV	ccttctccctcaatctcgaactcgtgtcctgtgacgc	37
HSRFP-17RV	tccctccatcttgaccttaaatctcataaactctttgatgacatcctcg	50
HSRFP-18RV	gagctggccattgtgagtttggccatgggtgagcttc	36

2.5. Characterization and analytical ultracentrifugation of purified mRFPs

Absorption spectra were measured using a UV–VIS spectrophotometer (Ultrospec 2000, Amersham Pharmacia Biotech), and fluorescence spectra with a FluoroMax-2 spectrofluorimeter (Jobin Yvon Horiba, Munich, Germany) at room temperature in 10-mm quartz cuvettes. For quantum yield determination, the fluorescence intensities of protein solutions of mRFPPruby were compared with fluorescence intensities of solutions of mRFP1 and mRFPmars (fluorescence quantum yield: 0.25) [10,11] in 100 mM potassium phosphate, pH 7.0.

Analytical ultracentrifugation experiments were performed with an analytical ultracentrifuge (Optima XL-A, Beckman Instruments, Palo Alto, CA) equipped with absorbance optics. Aluminum double sector

cells equipped with quartz windows were used throughout. The partial specific volume was estimated from the amino acid composition yielding a value of 0.7319 ml g<sup>-1</sup> for mRFPPruby [18].

Sedimentation equilibrium experiments were performed with 50 mM Tris–hydrochloride, pH 7.5, containing 100 mM potassium chloride and 0.4 mg of protein per ml at 17500 rpm and 4 °C.

2.6. Cloning of mRFPPruby-β-actin

A modified pcDNA3 expression vector (Invitrogen, Karlsruhe, Germany) containing GFP-human-β-actin under control of an human β-actin promoter (PAGA) was a gift of Bernhard Wehrle-Haller (Geneva, Switzerland), and was used to construct a corresponding mRFP vector. The GFP-encoding sequence was replaced by both humanized mRFP sequences (mRFPmars and mRFPPruby).



Fig. 1. Construction of a humanized mRFPmars. (A) Assembly of 36 oligonucleotides for the construction of a synthetic humanized version of mRFPmars. 5' and 3' overhangs including restriction sites for the cloning into pNCO113 (*Eco*RI and *Bgl*II, underlined), and for the generation of fusion proteins in eukaryotic vector systems (*Hind*III and *Bam*HI, boxed) were added to the coding region of mRFPmars. HSRFP-1FW to 18FW, forward oligonucleotides; HSRFP-1RV to 18RV, reverse oligonucleotides. (B) Top: Positions of the converted amino-acid residues superimposed on the X-ray structure of DsRed adopted from Yarbrough et al. [22]. The DsRed chromophore is drawn in yellow, the six mutated residues leading to mRFPmars [11] are drawn in green; the four mutated residues leading to the enhanced version of mRFPmars, designated mRFPPruby, are drawn in red. Three of four residues mutated in mRFPPruby are located on the surface of the protein. The amino acid exchange A57S is located within the structure. Below: Sequence comparison of mRFPPruby (this study), mRFPmars [11], mRFP1 [10] and DsRed [8].

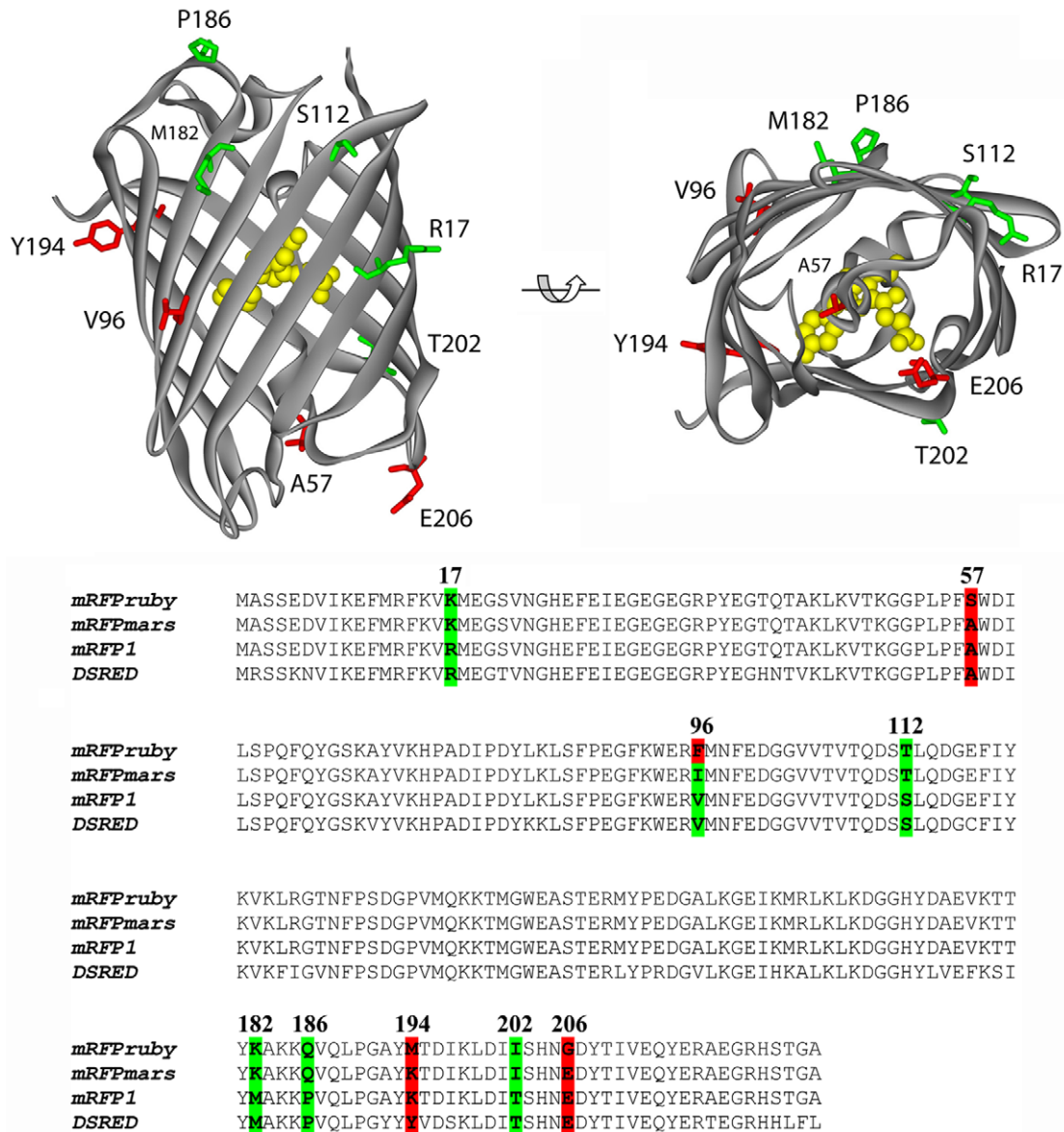


Fig. 1 (continued)

### 2.7. Transfection of mammalian cell lines

NIH 3T3 mouse fibroblasts were obtained from the American Type Culture Collection. Immortalized mouse chondrocytes were a kind gift from Professor Reinhard Fässler (Martinsried, Germany). All cell lines were maintained in DMEM supplemented with 10% fetal calf serum (Invitrogen, Karlsruhe, Germany). Cells were transiently transfected using Lipofectamine 2000 (Invitrogen) according to the manufacturer's protocol at a DNA:reagent ratio of 1:2.5 and assessed for expression of fluorescent proteins by video microscopy and/or FACS analysis 24–32 h after transfection.

### 2.8. FACS analysis of transfected cell cultures

For flow cytometry, transfected cells were trypsinized and washed twice in PBS containing 1% bovine serum albumin. FACS analysis was performed on a FACSCalibur system (Becton Dickinson, Franklin Lakes, NJ) using CellQuest Pro software (Becton Dickinson).

### 2.9. Microscopy

For video microscopic observations, transfected cells were seeded onto glass bottom culture dishes (MatTek, Ashland, MA) pre-coated with 10 µg/ml bovine plasma fibronectin (Calbiochem, San Diego,

CA) in PBS. Live cells were recorded using a Zeiss Axiovert 300M inverted microscope equipped with a CCD camera (Roper Scientific, Duluth, GA) and a stage incubator (EMBL Precision Engineering, Heidelberg, Germany). MetaMorph software (Molecular Devices, Downingtown, PA) was used for microscope control and image acquisition.

## 3. Results

### 3.1. Synthesis of humanized versions of mRFP

The gene coding for a humanized version of mRFPmars [11] was synthesized by oligonucleotide assembly and subsequent PCR amplification (Fig. 1A). Thirty-six oligonucleotides were employed to assemble the synthetic mRFPmars gene that was optimized for expression in human cells by replacement of 153 codons and thereby triggering the GC-content to 50.2%. The synthetic DNA fragment was cloned into the bacterial expression vector pNCO113 [15].

Colonies were screened on the basis of maturation behaviour and brilliance, and the coding sequences were monitored by DNA sequencing. During the process of screening, one mutant, HS-mRFPmars-7, further designated as mRFPPruby, was found to be more brilliant and to mature faster in *E. coli* cells than the original mRFPmars clone. Gene analysis of the mRFPPruby variant indicated that the mutated protein has four additional exchanges, A57S, I96F, K194M, and E206G, as compared to the mRFPmars amino acid sequence. Three of the four mutations are located on the surface of the protein, A57S lies within the structure (Fig. 1B).

The recombinant *E. coli* strains carrying the synthetic gene variants under the control of a T5 promoter and lac operator produced a 27.5 kDa protein that constituted approximately 10% of the total protein mass when using the conditions for expression described in Section 2. Both humanized mRFP variants, mRFPmars and mRFPPruby, were purified by hydrophobic interaction chromatography followed by anion exchange and gel filtration chromatography. The purified proteins appeared homogeneous (MW 27.5 kDa) as judged by sodium dodecyl polyacrylamide gel electrophoresis, in agreement with sedimentation equilibrium experiments indicating a molecular mass of 27 kDa using an ideal monodisperse model for calculation (Fig. 2). Compared with the calculated molecular mass of 27.5 kDa, the experimental data are in agreement with mRFPPruby having a monomeric quaternary structure.

The absorbance and emission spectra of humanized mRFPmars and mRFPPruby showed no significant differences (Fig. 3), and are almost identical to the previously published absorbance spectra of mRFP1 [10] and *Dictyostelium* mRFPmars [11]. The extinction coefficient ( $\epsilon$ ) for mRFPPruby at 585 nm

was  $32297 \text{ M}^{-1} \text{ cm}^{-1}$ . An pH dependency of the shorter wavelength absorption peak at 503 nm and the corresponding emission peak at 515 nm as described previously for the spectra of *Dictyostelium* mRFPmars [11] and mRFP1 [10], was detected also for both the spectra of humanized mRFPmars and mRFPPruby (data not shown). The determined fluorescence quantum yield for mRFPPruby (0.25) was identical to that of mRFP1 and mRFPmars.

### 3.2. mRFPPruby used as fluorescent tag in mouse cells

mRFPPruby-labeled  $\beta$ -actin was expressed transiently in different mouse cell lines. Transfected mouse 3T3 fibroblasts expressing high levels of mRFPPruby- $\beta$ -actin could be detected by fluorescence activated cell sorting (FACS) analysis using a 488-nm excitation laser line, and were sorted demonstrating the usefulness of mRFPPruby for flow cytometry applications using standard instrumentation (Fig. 4A). In addition, the expression of the mRFPPruby-tagged actin was confirmed by Western blotting (Fig. 4B).

The detailed examination of mRFPPruby- $\beta$ -actin transfected cells by fluorescence microscopy revealed that the cytoskeletal actin structures visualized are comparable to the ones observed when using a well established GFP- $\beta$ -actin construct [19]. Bright fluorescence from mRFPPruby was evident in F-actin-rich structures such as stress fibers and lamellipodia as well as dot-like structures (Fig. 5), and fluorescently tagged actin in these structures showed similar dynamics in live-cell time lapse recordings as established by previous live-cell imaging studies using GFP- $\beta$ -actin in these cells (Movie 1 in Supplementary Material). Additionally, enrichment of mRFPPruby-labeled  $\beta$ -actin was prominent in the perinuclear space where cellular G-actin is abundant. Abnormal, aggregated actin, a common artifact with previous DsRed-based fluorescence tags, were observed only in cells expressing very high levels of mRFPPruby- $\beta$ -actin.

### 3.3. Double labeling studies using mRFPPruby and green fluorescent markers

To further assess the correct localization of mRFPPruby- $\beta$ -actin and its suitability for double labeling studies, we performed two sets of experiments. First, a mouse cell line (profilin fl/fl immortalized chondrocytes) stably transduced with GFP- $\beta$ -actin was transfected with mRFPPruby- $\beta$ -actin. Both signals showed an almost perfect colocalization (Fig. 6A–C), confirming that mRFPPruby- $\beta$ -actin localizes as well as GFP- $\beta$ -actin. From this result, we also conclude that neither of the fluorescence tagged actin forms is preferentially incorporated into any actin structure.

Second, we co-transfected NIH 3T3 fibroblasts with both mRFPPruby- $\beta$ -actin and a well-established GFP-tensin construct [20]. Tensin is an F-actin binding protein that localizes to fibrillar adhesions which are adhesion complexes formed by cells adhering to fibronectin. Fibrillar adhesions are anchored to actomyosin stress fibers. We investigated cells expressing a combination of mRFPPruby- $\beta$ -actin and GFP-tensin to visualize simultaneously the entire actin cytoskeleton and fibrillar adhesions (Fig. 6D–F). Furthermore, we could readily visualize the formation of fibrillar adhesions partially overlapping with actin bundles and record their dynamics in time-lapse movies (not shown), confirming the suitability of mRFPPruby for functional double labeling studies. These initial

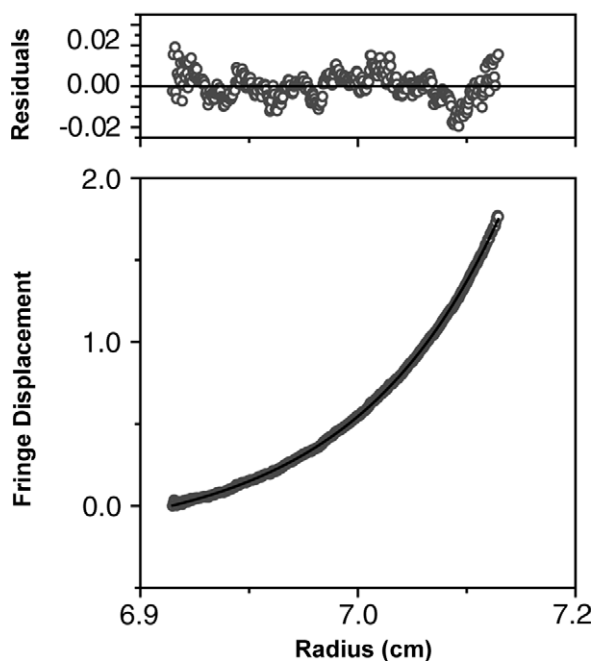


Fig. 2. Sedimentation equilibrium centrifugation of mRFPPruby. Protein concentration was monitored photometrically at 280 nm. The partial specific volume was estimated from the amino acid composition yielding a value of  $0.7319 \text{ ml g}^{-1}$  for mRFPPruby. Experiments were performed with 50 mM Tris-hydrochloride, pH 7.5, containing 100 mM potassium chloride and 0.4 mg of protein per ml at 17500 rpm and 4 °C. Residuals are shown at the top.

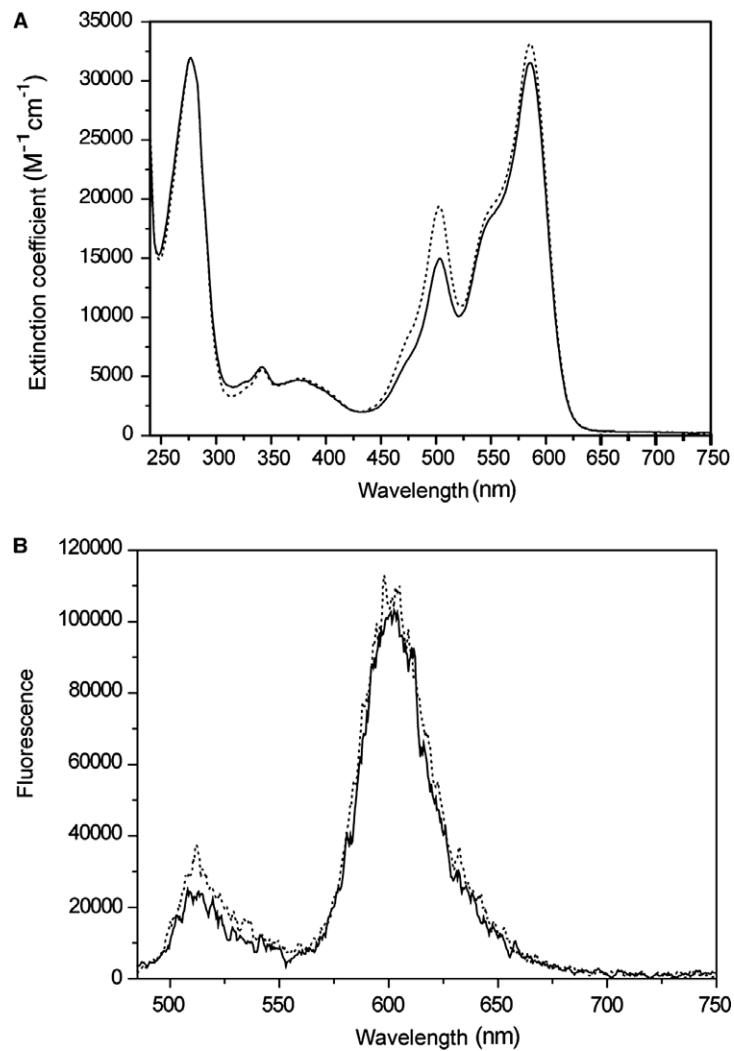


Fig. 3. Spectral properties of equal concentrations of mRFPruby (solid line) and humanized mRFPmars (dotted line) in 100 mM potassium phosphate, pH 7.0. (A) Absorption spectra. (B) Emission spectra. The excitation wavelength was 480 nm.

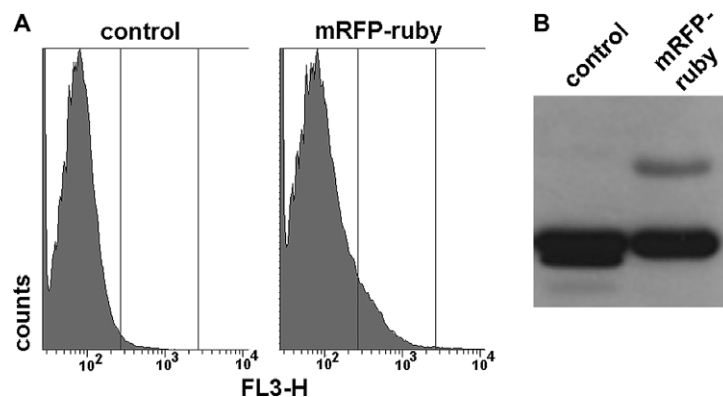


Fig. 4. Expression of mRFPruby-tagged  $\beta$ -actin in mammalian cells. (A) FACS profiles show fluorescence emission at 515–545 nm of untransfected control and mRFPruby- $\beta$ -actin-transfected 3T3 fibroblasts excited with a 488 nm laser line. Transfected cells are clearly detected as a broad peak shoulder. (B) Western blot of untransfected control and mRFPruby- $\beta$ -actin-transfected 3T3 fibroblasts lysates probed with an anti-actin antibody. Equal amounts of cell lysates were loaded per lane. Endogenous actin is detected as a prominent band at 42 kDa; below the 42 kDa band a degradation product is sometimes observed. mRFPruby- $\beta$ -actin is labeled as a less intense band of approximately 70 kDa.

studies demonstrate the usefulness of the mRFPruby variant for dual-color labeling experiments aiming to elucidate dynamic processes like the ones involved in regulation of actin polymerization.

#### 4. Discussion

In this study we report the development and testing of a new humanized mRFP variant, mRFPruby, which was opti-

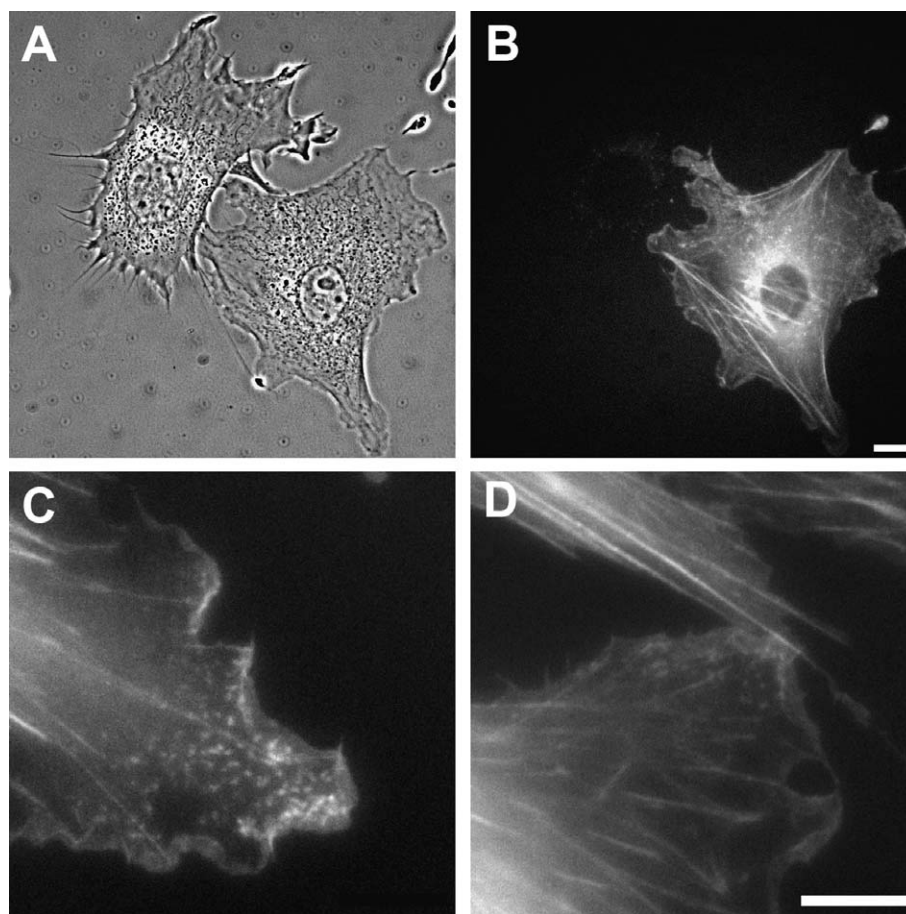


Fig. 5. Visualization of cytoskeletal structures using mRFPruby- $\beta$ -actin. (A) Phase contrast and (B) fluorescence image of NIH 3T3 fibroblasts transfected with mRFPruby- $\beta$ -actin. Stress fibers and lamellipodia are prominently labeled in the transfected cell. (C, D) Detailed views of 3T3 fibroblasts transfected with mRFPruby- $\beta$ -actin showing actin structures characteristic of lamellipodia. The leading edge, punctate focal complexes and nascent stress fibers can be distinguished. Bars: 10  $\mu$ m.

mized for the expression in mammalian cells. The biased codon usage in the construct expressing the previously introduced brilliant RFP, mRFPmars [11] – which was optimized for *Dictyostelium* – hampered the expression of the gene in mammalian cells. Vertebrates use codons that in most cases are rarely used in prokaryotic or other eukaryotic organisms and vice versa. Therefore, based on the preferred codon usage of *H. sapiens*, we re-engineered the mRFPmars-encoding gene without affecting the encoded amino acid sequence of the fluorescent protein. The *in vitro* gene synthesis was based on oligonucleotide assembly and subsequent PCR amplification. Insufficient fidelity of the DNA polymerase and the oligonucleotides used for the construction of the synthetic gene afforded a library of mRFPmars mutant proteins with different properties in terms of maturation behaviour and brilliance. One of these clones encoding mRFPruby was found to be more brilliant and to mature faster in the *E. coli* host as compared to the intended original variant, mRFPmars. Sequence analysis of mRFPruby revealed four amino acid changes not affecting the quaternary structure of the protein as proved by analytical ultracentrifugation. Interestingly, these mutations mainly located on the surface of the protein probably give rise to the enhanced fluorescence observed with this new mRFP variant upon expression *in vivo*.

Although various red fluorescent proteins are now available from different sources [5], their suitability has often not been assessed in live cell imaging studies. This is incongruous, since the usefulness of a fluorescent protein in imaging studies relies on its activity and compatibility in living cells. The functionality of a fluorescent protein is determined by a number of variables, some of which are difficult to quantify, including maturation time, photostability, toxicity, and brightness. These parameters are of course important, but do not always adequately describe how well a fluorescent protein will be expressed or fluorescence in a given cell. It has actually been demonstrated that the relative brightness of different DsRed variants in a cellular environment does not necessarily follow the order determined by *in vitro* spectroscopy [21]. Therefore, it is also important to thoroughly test fluorescent proteins empirically in a variety of cellular systems and applications.

The palette of fluorescent proteins now enables dual-color labeling investigations with sharp discrimination of the emission wavelengths especially when combinations of green (GFP) and red (RFP) fluorescent proteins are employed. Our results demonstrate that mRFPruby is a reliable fluorophore for live microscopy of mammalian cells. mRFPruby expressed in combination with  $\beta$ -actin yielded bright, stable fluorescence combined with low cytotoxicity both alone or in combination with GFP-tagged proteins and thus enabled the imaging of

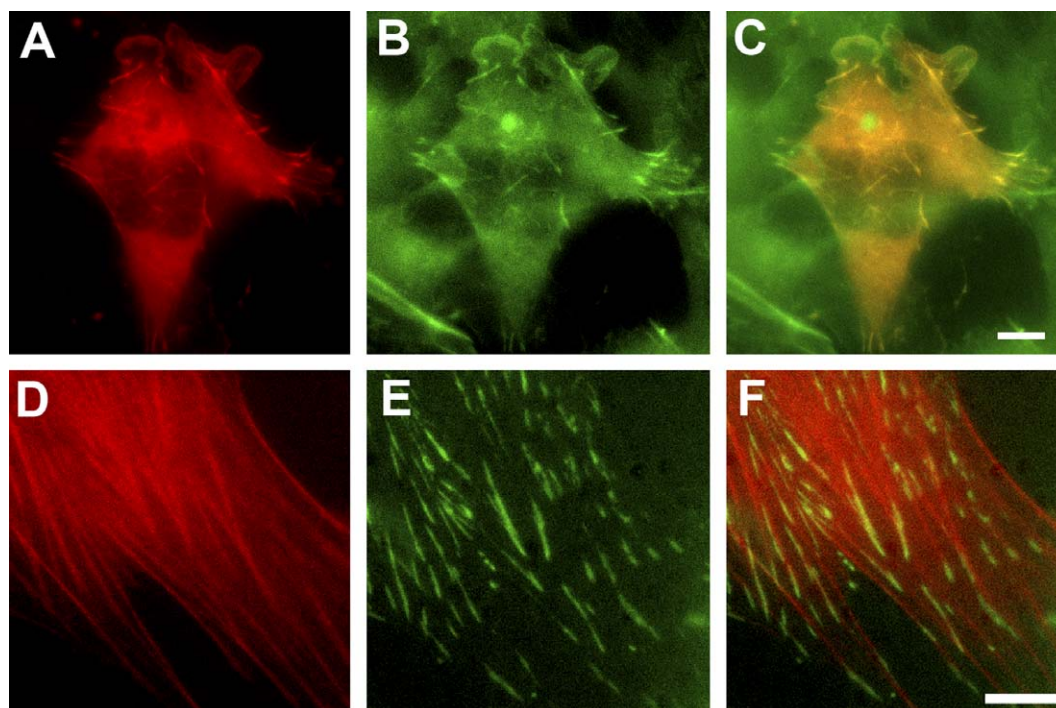


Fig. 6. Dual color-imaging using mRFPruby- $\beta$ -actin in combination with green fluorophores. (A–C) Immortalized mouse chondrocytes stably transduced with GFP- $\beta$ -actin (B) were transfected with mRFPruby- $\beta$ -actin (A). Both fluorophores colocalize as seen in the merged image (C). (D–F) 3T3 fibroblasts were co-transfected with mRFPruby- $\beta$ -actin (D) and GFP-tensin (E). Note the typical elongated fibrillar adhesions along stress fibers. The merged image is shown in (F) and colocalization is indicated by the yellow color. Bars: 10  $\mu$ m.

cytoskeletal structures. The fluorescence of mRFPruby is rather photo-stable and also offers the possibility to record dynamic processes such as cytoskeletal dynamics over time. To sum up, mRFPruby extends the repertoire of RFPs applicable for imaging studies in mammalian cells and might prove useful also in other combinations.

**Acknowledgments:** We thank Reinhard Fässler and Günther Gerisch (both Max-Planck-Institut für Biochemie, Martinsried), and Michael Schleicher (Ludwig-Maximilians-Universität München) for continuous support, Diane C. Lin and Shin Lin (Irvine, CA, USA) for their kind permission to use the GFP-tensin expression vector, and Michael Sixt (Max-Planck-Institut für Biochemie, Martinsried) for help during the FACS analysis. This work was supported by grants from the Deutsche Forschungsgemeinschaft (SFB 413), and Fonds der Chemischen Industrie to M.F.

#### Appendix A. Supplementary data

Supplementary data associated with this article can be found, in the online version, at doi:10.1016/j.febslet.2006.03.082.

#### References

- Miyawaki, A., Sawano, A. and Kogure, T. (2003) *Nat. Cell Biol.* (Suppl.), S1–S7.
- Lippincott-Schwartz, J. and Patterson, G.H. (2003) *Science* 300, 87–91.
- Tsien, R.Y. (1998) *Annu. Rev. Biochem.* 67, 509–544.
- Zhang, J., Campbell, R.E., Ting, A.Y. and Tsien, R.Y. (2002) *Nat. Rev. Mol. Cell Biol.* 3, 906–918.
- Shaner, N.C., Steinbach, P.A. and Tsien, R.Y. (2005) *Nat. Meth.* 2, 905–909.
- Baird, G.S., Zacharias, D.A. and Tsien, R.Y. (2000) *Proc. Natl. Acad. Sci. USA* 97, 11984–11989.
- Mizuno, H., Sawano, A., Eli, P., Hama, H. and Miyawaki, A. (2001) *Biochemistry* 40, 2502–2510.
- Matz, M.V., Fradkov, A.F., Labas, Y.A., Savitsky, A.P., Zaraisky, A.G., Markelov, M.L. and Lukyanov, S.A. (1999) *Nat. Biotechnol.* 17, 969–973.
- Knop, M., Barr, F., Riedel, C.G., Heckel, T. and Reichel, C. (2002) *Biotechniques* 33, 592–602.
- Campbell, R.E., Tour, O., Palmer, A.E., Steinbach, P.A., Baird, G.S., Zacharias, D.A. and Tsien, R.Y. (2002) *Proc. Natl. Acad. Sci. USA* 99, 7877–7882.
- Eichinger, L. et al. (2005) *Nature* 435, 43–57.
- Fischer, M., Haase, I., Simmeth, E., Gerisch, G. and Müller-Taubenberger, A. (2004) *FEBS Lett.* 577, 227–232.
- Diez, S., Gerisch, G., Anderson, K., Müller-Taubenberger, A. and Bretschneider, T. (2005) *Proc. Natl. Acad. Sci. USA* 102, 7601–7606.
- Nakamura, Y., Gojobori, T. and Ikemura, T. (2000) *Nucleic Acids Res.* 28, 292.
- Stueber, D., Matile, H. and Garotta, G. (1990) *Immunological Methods IV* (Lefkovits, I. and Pernis, P., Eds.), pp. 121–125.
- Bullock, W.O., Fernandez, J.M. and Short, J.M. (1987) *BioTechniques* 5, 376–379.
- Zamenhof, P. and Villarejo, M. (1972) *J. Bacteriol.* 110, 171–178.
- Laue, T.M., Shah, B.D., Ridgeway, T.M. and Pelletier, S.L. (1992) in: *Analytical Ultracentrifugation in Biochemistry and Polymer Science* (Harding, S.E., Rowe, A.J. and Horton, J.C., Eds.), pp. 90–125, Royal Society of Chemistry, Cambridge.
- Ballestrem, C., Wehrle-Haller, B. and Imhof, B.A. (1998) *J. Cell Sci.* 111, 1649–1658.
- Zamir, E., Katz, M., Posen, Y., Erez, N., Yamada, K.M., Katz, B.Z., Lin, S., Lin, D.C., Bershadsky, A., Kam, Z. and Geiger, B. (2000) *Nat. Cell Biol.* 2, 191–196.
- Robinson, L.C. and Marchant, J.S. (2005) *Biophys. J.* 88, 1444–1457.
- Yarbrough, D., Wachter, R.M., Kallio, K., Matz, M.V. and Remington, S.J. (2001) *Proc. Natl. Acad. Sci. USA* 98, 462–467.